# MmWave-NOMA-Based Semi-persistent Scheduling for Enhanced V2X Services

Fanwei Shi(✉), Bicheng Wang, Ruoqi Shi, Jian Tang, and Jianling Hu

School of Electronic and Information Engineering, Soochow University, Suzhou, China
fwshi@qq.com, jlhu@suda.edu.cn

**Abstract.** This paper investigates the semi-persistent scheduling (SPS) strategy for enhanced vehicle-to-everything (eV2X) services, which aims to meet the low latency and high reliability (LLHR) demands. To increase available spectrum and improve resource utilization, millimeter wave (mmWave) and non-orthogonal multiple access (NOMA) are considered. We first formulate the optimization problem of scheduling and resource allocation to minimize the SPS period. To solve this problem, the LLHR power control algorithm is proposed to provide evaluation indicators for user scheduling. Then, the beam division and user clustering algorithm is designed to reduce the complexity of the matching between users and resource blocks. After that, the matching problem with peer effects is solved by the proposed union-based matching algorithm. Complexity analysis is presented, and simulation results show that the scheduling period of eV2X systems can be improved by the proposed SPS strategy compared with the conventional mmWave SPS schemes.

**Keywords:** NOMA · mmWave · eV2X · Hybrid precoding · Semi-persistent scheduling

## 1 Introduction

Intelligent transport system (ITS) has been one of the highly concerned transmission systems, since it can provide security, transport efficiency and energy conservation [1]. To meet the requirements of the fifth generation (5G) ITS, the 3rd generation partnership project (3GPP) has proposed the enhanced vehicle-to-everything (eV2X) networks [2], which contains two interfaces [3], i.e. PC5 interface for sidelink (SL) and Uu interface for downlink/uplink (DL/UL). A typical type of eV2X services, e.g. advanced driving, is called time-triggered service, since it has obvious periodicity. Semi-persistent scheduling (SPS) has been proven to be better for time-triggered services than dynamic scheduling (DS), since it can reduce the signaling overhead [4]. However, eV2X networks also require a higher data rate, e.g. Gbps, than before [5].

To handle this challenge, millimeter waves (mmWave), e.g. 30 GHz and 63 GHz [6], are considered for eV2X networks. The shorter wavelengths facilitate the deployment of large-scale antenna system, which can improve the beamforming gain [7]. Typically, to achieve a balance between radio frequency (RF)


H. Gao et al. (Eds.): ChinaCom 2019, LNICST 312, pp. 193–206, 2020.
https://doi.org/10.1007/978-3-030-41114-5_15

chain overhead and transmission performance, hybrid precoding is proposed for mmWave systems [8]. Many advantages do the mmWave V2X systems have, but they also suffer from several drawbacks. For instance, the Doppler effect causes carrier frequency offset (CFO) in V2X systems.

Benefit from the non-orthogonal nature in frequency domain, power-domain non-orthogonal multiple access (NOMA) has been considered to solve the problem of CFO and frequent handovers of mmWave cells caused by vehicle mobility [9,10]. Moreover, the pairing-based NOMA can achieve the spectral efficiency about 30% higher than orthogonal multiple access (OMA) with a given bandwidth [11], which facilitates the transmission of large packets. Specifically, [12] designed a joint precoding and dynamic power control schemes for mmWave-NOMA systems with lens antenna arrays; [13] and [14] investigated the user selection and power allocation scheme for mmWave-NOMA networks. However, the above solutions [12–14] are designed to maximize system throughput for conventional cellular networks. Different from them, the key performance indicator (KPI) of eV2X systems is considered to be latency [3]. Therefore, the low latency and high reliability (LLHR) eV2X networks need a novel design of mmWave-NOMA schemes.

Specifically, we design a mmWave-NOMA-based SPS scheme for DL. The existing researches like [15] were also directed at DL. Note that eV2X systems prefer to utilize the least number of RBs to serve all VUEs in coverage under the constraints of quality of service (QoS), which is different from the event-triggered services in conventional cellular systems. This view was also reflected in [16], where a centralized SPS strategy is designed for machine-type communications (MTC) to minimize the system bandwidth. Specially, for eV2X system, the minimization of SPS period is more flexible and reasonable, since the users have a uniform constraint of latency and realiability [3].

The rest of the paper is organized as follows. In Sect. 2, the system model is described and the SPS problem is formulated. In Sect. 3, the SPS strategy is designed and analyzed. Specifically, the LLHR power control (LLHR-PC) algorithm, the beam division and VUE clustering (BD&VC) algorithm, and union-based VUE-RB matching algorithm is proposed respectively. Finally, simulation results are presented in Sect. 4 and conclusions are drawn in Sect. 5.

## 2 System Model and Problem Formulation

### 2.1 Scenario Description

Figure 1 shows the considered mmWave-NOMA-based cellular eV2X system, where base station (BS) is equipped with $M_{BS}$ transmit antennas and $G_{BS}$ RF chains. Each VUE is equipped with single antenna. Each RF chain is connected to all antennas to form a fully connected structure [8].

The VUE set of the $n$-th cluster in the $g$-th beam is expressed as $\mathcal{N}_{g,n}$, which contains no more than two VUEs $V_{g,n}^{i}$, $i = 1, 2$ [18]. $|\mathcal{N}_{g,n}|$ represents the number of elements in the set $\mathcal{N}_{g,n}$. Hence, $|\mathcal{N}_{g,n}| \leq 2$ and $\mathcal{N}_{g,n} \cap \mathcal{N}_{g',n'} = \phi$ for $|g - g'| + |n - n'| \neq 0$. An adaptive NOMA/OMA clustering is considered

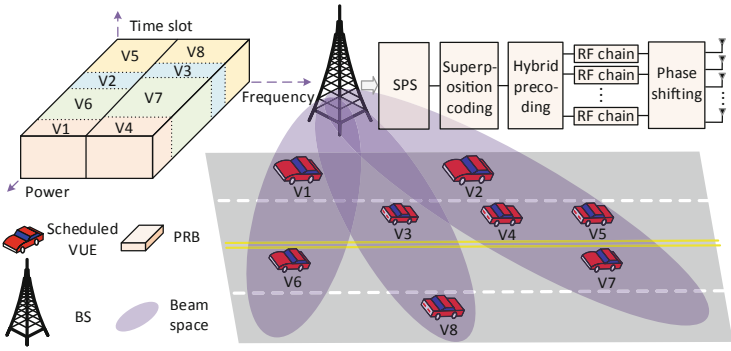


**Fig. 1.** System model of Cellular V2X transmission.

in this system, since one beam may have an odd number of VUEs. Specifically, NOMA is adopted when $|\mathcal{N}_{g,n}| = 2$, while OMA is adopted when $|\mathcal{N}_{g,n}| = 1$. Without loss of generality, assume that the channel gain of $V^1_{g,n}$ is stronger than $V^2_{g,n}$. The cluster set of the $g$-th beam is expressed as $\mathcal{N}_g$, which satisfies $|\mathcal{N}_g| = \lceil (\sum_n |\mathcal{N}_{g,n}|)/2 \rceil$. Hence, the number of VUEs and the number of clusters are respectively $U = \sum_{g=1}^{G_D} \sum_{n=1}^{|\mathcal{N}_g|} |\mathcal{N}_{g,n}|$ and $|\mathcal{N}| = \sum_{g=1}^{G_D} |\mathcal{N}_g|$, where $G_D$ is the number of formed beams, $G_D \leq G_{BS}$.

Particularly, the bandwidth of each RB is defined as the DL aggregate system bandwidth $\omega$, and the width of time slot is $\tau_{RB}$. One SPS period requires $K$ time slots to finish the transmission of packets under the QoS constraints, i.e., the SPS period is $K\tau_{RB}$.

### 2.2 Channel Model

We adopt the channel model widely used in mmWave systems [12–15]. The channel vector of $V^i_{g,n}$ is

$$\mathbf{h}^i_{g,n} = \sqrt{M_{BS}} \sum\nolimits_{l=1}^{L} \beta^i_{g,n,l} \mathbf{a}\left(\phi^i_{g,n}\right), \tag{1}$$

where $L$ is the number of paths from BS to each VUE. $\beta^i_{g,n,l}$ is the complex Gaussian gain of $V^i_{g,n}$ in the $l$-th path, and $\beta^i_{g,n,l} \sim \mathcal{CN}(0, \ell^i_{g,n,l})$. $\ell^i_{g,n,l}$ is the average path loss from BS to $V^i_{g,n}$. Considering the mobility of VUEs, we have $\ell^i_{g,n,l} = |\mathbf{d}^i_{g,n} + \mathbf{v}^i_{g,n} t_w|^{-\eta_l}$, where $\mathbf{d}^i_{g,n}$ and $\mathbf{v}^i_{g,n}$ are the displacement vector and relative velocity between BS and $V^i_{g,n}$, respectively. $t_w$ is the waiting interval, and the maximum can be $t_w = K\tau_{RB}$. $\eta_l$ is the path loss exponent of the $l$-th path.

$\mathbf{a}(\phi^i_{g,n})$ represents the array steering vector, and $\phi^i_{g,n}$ represents the azimuth angle of departure (AoD). Particularly, the uniform linear array (ULA) is adopted, and $\mathbf{a}(\phi^i_{g,n})$ can be expressed as

$$\mathbf{a}(\phi^i_{g,n}) = {M_{BS}}^{-\frac{1}{2}} [e^{\frac{j2\pi \mathbf{m} f_c d \sin(\phi^i_{g,n})}{c}}]^T, \tag{2}$$

where $f_c$, $c$, $d$ and $\mathbf{m} = \{0, 1, \ldots, M_{BS} - 1\}$ are respectively the carrier center frequency (CCF), the speed of light, the antenna spacing and the antenna set.

### 2.3 Transmitting and Receiving

Considering the analog precoder with $B$ bits quantization precision, the minimum step of phase shifter is $2^{1-B}\pi$. Combined with the channel feature of ULA, the analog precoding vector $\mathbf{w}_g^a$ satisfies

$$\mathbf{w}_g^a \in \mathcal{W}^a = \left[\mathbf{a}\left(2^{1-B}\pi\mathbf{b}\right)\right], \tag{3}$$

where $\mathbf{b} = \left\{0, 1, \ldots, 2^B - 1\right\}$ represent phase shift set, and $\mathbf{w}_g^a$ is the analog precoding vector of the $g$-th beam. Hence, the analog precoding matrix can be expressed as

$$\mathbf{W}^a = \left[\mathbf{w}_1^a, \mathbf{w}_2^a, \ldots, \mathbf{w}_{G_D}^a\right]. \tag{4}$$

Then, the digital precoding vector $\mathbf{w}_{g,n}^i$ of $V_{g,n}^i$ is calculated. The adopted zero-forcing digital precoding scheme is given by

$$\tilde{\mathbf{W}}^d = (\mathbf{W}^a)^H \mathbf{H}\Big(\mathbf{H}^H \mathbf{W}^a (\mathbf{W}^a)^H \mathbf{H}\Big)^{-1}, \tag{5}$$

where the channel matrix is $\mathbf{H} = [\mathbf{h}_{1,1}^1, \ldots, \mathbf{h}_{2,1}^1, \ldots]$, containing the channel vectors of all VUEs. The digital precoding matrix is $\tilde{\mathbf{W}}^d = [\tilde{\mathbf{w}}_{1,1}^1, \ldots, \tilde{\mathbf{w}}_{2,1}^1, \ldots]$.

After normalization, $\mathbf{w}_{g,n}^i$ can be expressed as

$$\mathbf{w}_{g,n}^i = \tilde{\mathbf{w}}_{g,n}^i / \left\|\tilde{\mathbf{w}}_{g,n}^i\right\|. \tag{6}$$

To facilitate the expression of signal, we define a scheduling indicator $\theta_{g,n}^k$ for the VUEs in $\mathcal{N}_{g,n}$, where

$$\theta_{g,n}^k = \begin{cases} 1, \text{ if } \mathcal{N}_{g,n} \text{ is scheduled in the k - th PRB,} \\ 0, \text{ otherwise.} \end{cases} \tag{7}$$

Then, the received signal of $V_{g,n}^i$ in the $k$-th RB can be expressed as

$$y_{g,n}^{i(k)} = \sqrt{P_t}\bar{\mathbf{h}}_{g,n}^i \sum_{x=1}^{G_D} \sum_{y=1}^{|\mathcal{N}_x|} \sum_{z=1}^{|\mathcal{N}_{x,y}|} \mathbf{w}_{x,y}^z \sqrt{\theta_{x,y}^k \alpha_{x,y}^z} x_{x,y}^z + v_{g,n}^i, \tag{8}$$

where $\bar{\mathbf{h}}_{g,n}^i = (\mathbf{h}_{g,n}^i)^H \mathbf{W}^a$. $P_t$ represents the transmit power, and $v_{g,n}^i$ represents the additive noise with a power spectral density of $\sigma_v$. $\alpha_{g,n}^i$ is the power allocation factor, which satisfies

$$\sum\nolimits_{g=1}^{G_D} \sum\nolimits_{n=1}^{|\mathcal{N}_g|} \sum\nolimits_{i=1}^{|\mathcal{N}_{g,n}|} \theta_{g,n}^k \alpha_{g,n}^i \leq 1, \tag{9}$$

where $k \in \{1, 2, \ldots K\}$. Minimum mean square error - successive interference cancellation (MMSE-SIC) is adopted to decode the received signal [11], where the mean square error (MSE) is given by

$$e^i_{g,n} = E[||\rho^i_{g,n} y^{i(k)}_{g,n} - \theta^k_{g,n} x^i_{g,n}||^2]. \tag{10}$$

$\rho^i_{g,n}$ represents the channel equalization coefficient (CEC) of $V^i_{g,n}$, and we assume $E\left[\left\|x^i_{g,n}\right\|^2\right] = 1$.

### 2.4 SPS Problem Formulation

The spectral efficiency for $V^i_{g,n}$ to transmit a packet of $L^i_{g,n}$ bytes is given by

$$\bar{R}^i_{g,n} = 8 \ln 2 \cdot \frac{L^i_{g,n}}{\tau_{RB}\omega}, \tag{11}$$

where nature unit is utilized as the unit of data to simplify calculations, and thus, the unit of $\bar{R}^i_{g,n}$ is $nats/(s \cdot Hz)$.

According to (8), the signal to interference plus noise ratio (SINR) of $V^i_{g,n}$ can be expressed as

$$\gamma^i_{g,n} = \frac{||\bar{\mathbf{h}}^i_{g,n} \mathbf{w}^i_{g,n}||^2 \theta^k_{g,n} \alpha^i_{g,n} P_{BS}}{P_t \sum\limits_{x \neq g} \sum\limits_{y=1}^{|\mathcal{N}_x|} \sum\limits_{z=1}^{|\mathcal{N}_{g,n}|} ||\bar{\mathbf{h}}^i_{g,n} \mathbf{w}^z_{x,y}||^2 \theta^k_{x,y} \alpha^z_{x,y} + \xi^i_{g,n} + \sigma^2_v}, \tag{12}$$

where $\xi^i_{g,n}$ represents the intra-beam interference. Since the clusters in the same beam cannot be multiplexed in the same RB, $\xi^i_{g,n}$ is also the intra-cluster interference, where

$$\xi^i_{g,n} = \begin{cases} P_t ||\bar{\mathbf{h}}^{(1)}_{g,n} \mathbf{w}^i_{g,n}||^2 \theta^k_{g,n} \alpha^{(1)}_{g,n}, & \text{if } |\mathcal{N}_{g,n}| = 2,\ i = 2, \\ 0, & \text{otherwise.} \end{cases} \tag{13}$$

Then, the achievable spectral efficiency of $V^i_{g,n}$ is

$$R^i_{g,n} = \ln(1 + \gamma^i_{g,n}). \tag{14}$$

Since latency is the goal of optimization, the QoS constraints are mostly concerned with reliability. In this paper, PRR is utilized to describe reliability [6], which is given by

$$\delta^i_{g,n} = (1 + e^{-\mu(R^i_{g,n} - \bar{R}^i_{g,n})})^{-1} \geq \delta_{th}, \tag{15}$$

where $\mu$ is the slope parameter [1], and $\delta_{th}$ represents the threshold of reliability in one SPS period.

Based on the above model, the time-frequency resource allocation and power control problem of the BS in one SPS period can then be formulated as,

$$\min_{\{\theta^k_{g,n}\}, \{\alpha^i_{g,n}\}} K\tau_{RB}, \tag{16}$$

$$s.t.\ (9), (15),$$

$$\alpha_{g,n}^{i} \geq 0, \forall 1 \leq g \leq G_D, 1 \leq n \leq |\mathcal{N}_g|, 1 \leq i \leq |\mathcal{N}_{g,n}|, \tag{16a}$$

$$\sum\nolimits_{k=1}^{K} \theta_{g,n}^{k} = 1, \forall 1 \leq g \leq G_D, 1 \leq n \leq |\mathcal{N}_g|, \tag{16b}$$

$$\sum\nolimits_{n=1}^{|\mathcal{N}_g|} \theta_{g,n}^{k} \leq 1, \forall 1 \leq g \leq G_D, 1 \leq k \leq K. \tag{16c}$$

The constraints of transmit power and QoS are described in constraints (9), (16a) and (15). Constraint (16b) represents that each cluster in each beam is scheduled once and only once in one SPS period, and thus, $\sum_{g=1}^{G_D} \sum_{n=1}^{|\mathcal{N}_g|} \sum_{k=1}^{K} \theta_{g,n}^{k} = |\mathcal{N}|$. The constraint (16c) represents that no more than one VUE in the same beam is scheduled in the same time slot.

As is shown in problem (16), the multiplexing in power domain and spatial domain increases the complexity. Hence, we split problem (16) into a power control process and a VUE-RB matching process, and design an iterative algorithm to solve the joint optimization problem of $\{\theta_{g,n}^{k}\}$ and $\{\alpha_{g,n}^{i}\}$.

## 3 MmWave-NOMA-Based SPS Strategy

### 3.1 Optimal LLHR Power Control

The premise of performing power control is that we have known the VUE-RB matching result, i.e., $\{\theta_{g,n}^{k}\}$ is determined. Hence, a temporary period $K\tau_{RB}$ is also known. For the $k$-th time slot, this sub-problem can be described as

$$\max_{\{\alpha_{g,n}^{i}\}} \min_{\{g,n,i\} \in \Gamma_k} \delta_{g,n}^{i}, \tag{17}$$

$$s.t. \alpha_{g,n}^{i} \geq 0, \tag{17a}$$

$$\sum\nolimits_{g=1}^{G_D} \sum\nolimits_{n=1}^{|\mathcal{N}_g|} \sum\nolimits_{i=1}^{|\mathcal{N}_{g,n}|} \theta_{g,n}^{k} \alpha_{g,n}^{i} \leq 1, \tag{17b}$$

where $\Gamma_k = \{g, n, i | \theta_{g,n}^{k} = 1, V_{g,n}^{i} \in \mathcal{N}_{g,n}\}$ represents the VUE set scheduled in the $k$-th time slot. The power constraint in the $k$-th time slot is shown in (17a) and (17b). Additionally, if the result $\{\alpha_{g,n}^{i}\}$ satisfies constraint (15), it can be one of the feasible solutions to problem (16), and thus, we can try to schedule another cluster in the $k$-th time slot to shorten SPS period, until constrain (15) cannot be satisfied.

According to (10), a MSE is generated when the received signal of $V_{g,n}^{i}$ is decoded by MMSE-SIC, which can be expressed as

$$e_{g,n}^{i} = |\rho_{g,n}^{i} \sqrt{P_t \theta_{g,n}^{k} \alpha_{g,n}^{i}} \bar{\mathbf{h}}_{g,n}^{i} \mathbf{w}_{g,n}^{i} - \theta_{g,n}^{k}|^2 + |\rho_{g,n}^{i}|^2 \varsigma_{g,n}^{i}, \tag{18}$$

where $\varsigma_{g,n}^{i}$ contains the intra-beam interference, the inter-beam interference and the additive noise. $\varsigma_{g,n}^{i}$ is formulated as

$$\varsigma_{g,n}^{i} = P_t \sum_{x \neq g} \sum_{y=1}^{|\mathcal{N}_x|} \theta_{x,y}^{k} \sum_{z=1}^{|\mathcal{N}_{g,n}|} ||\bar{\mathbf{h}}_{g,n}^{i} \mathbf{w}_{x,y}^{z}||^2 \alpha_{x,y}^{z} + \xi_{g,n}^{i} + \sigma_v^2. \tag{19}$$

By deriving $e_{g,n}^{i}$ with respect to $\rho_{g,n}^{i}$, we can get the optimal CEC when the minimum MSE is obtained,

$$\rho_{g,n}^{i} = 1 - \varsigma_{g,n}^{i} (\sqrt{P_t \theta_{g,n}^{k} \alpha_{g,n}^{i}} \bar{\mathbf{h}}_{g,n}^{i} \mathbf{w}_{g,n}^{i} + \varsigma_{g,n}^{i})^{-1}. \tag{20}$$

At this point, the MSE can be formulated as

$$E_{g,n}^{i} = \min_{\rho_{g,n}^{i}} e_{g,n}^{i} = \varsigma_{g,n}^{i} (\sqrt{P_t \theta_{g,n}^{k} \alpha_{g,n}^{i}} \bar{\mathbf{h}}_{g,n}^{i} \mathbf{w}_{g,n}^{i} + \varsigma_{g,n}^{i})^{-1}. \tag{21}$$

According to (21) and (14), $R_{g,n}^{i} = -\min_{\rho_{g,n}^{i}} \ln e_{g,n}^{i}$. Substituting it into the objective function of problem (17), we have

$$\delta_{g,n}^{i} = \max_{\rho_{g,n}^{i}} \frac{1}{1 + e^{\mu \bar{R}_{g,n}^{i}} \left(e_{g,n}^{i}\right)^{\mu}}. \tag{22}$$

However, the objective function of problem (17) is still non-convex with respect to $\{\alpha_{g,n}^{i}\}$. Hence, we then convert it into a convex problem. According to (22) and (15), we have

$$\max_{\rho_{g,n}^{i}} \frac{1}{1 + e^{\mu \bar{R}_{g,n}^{i}} \left(e_{g,n}^{i}\right)^{\mu}} \geq \delta_{th}, \tag{23}$$

Note that according to (20), the optimal CEC can be uniquely determined by $\{\alpha_{g,n}^{i}\}$ after $\{\theta_{g,n}^{k}\}$ is given. Therefore, constraint (15) can be formulated as

$$\varsigma_{g,n}^{i} - [e^{-\mu \bar{R}_{g,n}^{i}} (\tilde{\delta}_{th}^{-1} - 1)]^{\frac{1}{\mu}} (\sqrt{P_t \theta_{g,n}^{k} \alpha_{g,n}^{i}} \bar{\mathbf{h}}_{g,n}^{i} \mathbf{w}_{g,n}^{i} + \varsigma_{g,n}^{i}) \leq 0, \tag{24}$$

where $\tilde{\delta}_{th}$ is the PRR threshold of the current round in LLHR-PC algorithm. Then, problem (17) can be transferred into the following form,

$$\min_{\{\alpha_{g,n}^{i}\}} \sum\nolimits_{g=1}^{G_D} \sum\nolimits_{n=1}^{|\mathcal{N}_g|} \sum\nolimits_{i=1}^{|\mathcal{N}_{g,n}|} \theta_{g,n}^{k} \alpha_{g,n}^{i}, \tag{25}$$

$$s.t. (17a), (24).$$

In the proposed LLHR-PC algorithm shown in Algorithm 1, the optimal power allocation $\{\alpha_{g,n}^{i}\}$ is calculated for the $k$-th time slot. If the solution to problem (25) cannot satisfy constraint (17b) when $\tilde{\delta}_{th} = \delta_{th}$, the current matching $\{\theta_{g,n}^{k}\}$ is proven to be infeasible. Otherwise, we have $\tilde{\delta}_{th} \in [\delta_{th}, 1)$. In each round, a temporary PRR threshold $\tilde{\delta}_{th}$, is utilized to calculate $\{\alpha_{g,n}^{i}\}$, until the search space of $\tilde{\delta}_{th}$ is limited to $\varepsilon_{\delta}$.

**Algorithm 1.** Proposed LLHR-PC Algorithm

**Require:** $\{\theta_{g,n}^k\}$ of the $k$-th time slot.
**Ensure:** $\{\alpha_{g,n}^i\}$, $\delta_{LB}$.
1: Init. $\delta_{LB} = \delta_{th}$, $\delta_{UB} = 1$, $\tilde{\delta}_{th} = \delta_{LB}$;
2: Solve problem (25);
3: **if** $\sum_{g=1}^{G_D} \sum_{n=1}^{|\mathcal{N}_g|} \sum_{i=1}^{|\mathcal{N}_{g,n}|} \theta_{g,n}^k \alpha_{g,n}^i > 1$ or (25) is infeasible **then**
4: $\{\theta_{g,n}^k\}$ is infeasible;
5: **else**
6: **while** $\delta_{UB} - \delta_{LB} \geq \varepsilon_\delta$ **do**
7: $\tilde{\delta}_{th} = (\delta_{DB} + \delta_{UB})/2$ and solve problem (25);
8: **if** $\sum_{g=1}^{G_D} \sum_{n=1}^{|\mathcal{N}_g|} \sum_{i=1}^{|\mathcal{N}_{g,n}|} \theta_{g,n}^k \alpha_{g,n}^i \leq 1$ **then**
9: $\delta_{LB} = \tilde{\delta}_{th}$ and record $\{\alpha_{g,n}^i\}$;
10: **else**
11: $\delta_{UB} = \tilde{\delta}_{th}$;

### 3.2 Union-Based VUE-RB Matching

The following matching problem is formed and analyzed to calculate both $\{\theta_{g,n}^k\}$ and $\{\alpha_{g,n}^i\}$. Use two disjoint sets of $V$ and $F$ to respectively represent $U$ VUEs and $K$ RBs in an eV2X system, where $V = \{v_1, v_2, \ldots, v_U\}$, $F = \{f_1, f_2, \ldots, f_K\}$. The matching problem with respect to $V$ and $F$ can be described as follows.

*Definition 1. A matching $\Psi$ is a mapping from the set $V \cup F$ to the set $V \cup F$, where (1) $\Psi(v_i) \in F \cup \{v_i\}$; (2) $\Psi(f_k) \subset V \cup \{f_k\}$; (3) $\Psi(v_u) = f_k \Leftrightarrow v_u \in \Psi(f_k)$;*

Condition (1) implies that each VUE is scheduled in no more than one RB, i.e., $|\Psi(v_i)| = 1$ and $|\Psi(v_i) \cap F| \leq 1$, while condition (2) implies that each RB can serve several VUEs. Condition (3) indicates that the mapping between $v_k$ and $f_k$ is symmetrical. Specially, $\Psi(j) = \{j\}$ happens when there is no other matching for element $j$. Note that if $\exists j \in V \cup F$ such that $\Psi(j) = \{j\}$, the current matching $\Psi$ will be infeasible.

When $\Psi(v_u) = \Psi\left(v_u^{'}\right) = f_k$ and $v_u, v_u^{'} \in V$, the co-channel interference will occur between $v_u$ and $v_u^{'}$. Since the co-channel interference can be intra-beam or inter-beam, $\Psi$ suffers from more complex peer effects compared with the existing matching problem [4]. Hence, the preference $\mathcal{R}$ is formed to helps players search for other players by interesting.

*Definition 2. For two sets of VUEs $V^i, V^j \subseteq V$, $\mathcal{R}\left(V^i f_k V^j\right)$ represents that $f_k$ prefers $V^i$ than $V^j$, while for two sets of RBs $f_i, f_j \in F$, $\mathcal{R}(f_i v_u f_j)$ represents that $v_u$ prefers $f_i$ than $f_j$, which can be formulated as*

$$\mathcal{R}\left(V^i f_k V^j\right) \Leftrightarrow \tilde{\delta}_{th}\left(f_k, V^i\right) > \tilde{\delta}_{th}\left(f_k, V^j\right), \tag{26}$$

$$\begin{aligned}\mathcal{R}\left(f_i v_u f_j\right) \Leftrightarrow & \min\{\tilde{\delta}_{th}(f_i, \Psi(f_i) \cup v_u), \tilde{\delta}_{th}(f_j, \Psi(f_j)\} \\ & > \min\{\tilde{\delta}_{th}(f_i, \Psi(f_i)), \tilde{\delta}_{th}(f_j, \Psi(f_j) \cup v_u\}\end{aligned} \tag{27}$$

Note that the preference is transitive, and thus, a preference list can be formed by (26) and (27). A feasible $\Psi$ should satisfies that for $\forall v_u \in V$ and $\forall f_k \in F$, $\mathcal{R}\left(\Psi\left(f_k\right) f_k\{f_k\}\right)$ and $\mathcal{R}\left(\Psi\left(v_u\right) v_u\{v_u\}\right)$ are always established. Additionally, if $v_u$ and $v_u^{'}$ are in the same beam, $v_u^{'}$ can replace the position of $v_u$ in the RB. Such a relationship is called alternative.

**Algorithm 2.** Proposed BD&VC Algorithm

**Require:** $\mathcal{W}^a$; VUE set $V$; $\mathbf{h}_u$, $u \in \{1, 2, \ldots, U\}$.
**Ensure:** Cluster set $\mathcal{N}$; $G_D$; $\mathbf{W}^a$; $\{\mathbf{w}_{g,n}^i\}$.
1: Init. VUE set in each beam $\Gamma = \{\Gamma_1, \Gamma_2, \ldots, \Gamma_{G_{BS}}\}$, where $\Gamma_x = \varnothing$ for $x \in \{1, 2, \ldots, G_{BS}\}$; $\mathbf{W}^a = \varnothing$;
2: **for all** $u \in U$ **do**
3: $\quad g = \arg \max_{x \in G_{BS}} \left\{ \frac{\|\mathbf{h}_u^H \mathbf{w}_x^a\|}{\|\mathbf{h}_u\| \|\mathbf{w}_x^a\|} \right\}$; $\Gamma_g = \Gamma_g \cup v_u$;
4: $\mathbf{G} = \{x | \Gamma_x \neq \emptyset, 1 \leq x \leq G_{BS}\}$;
5: $G_D = |\mathbf{G}|$ and $\mathbf{W}_a = \bigcup_{g \in \mathbf{G}} \mathbf{w}_g^a$;
6: **for all** $g \in \mathbf{G}$ **do**
7: $\quad \mathrm{H} = \left\{ \left\| \mathbf{h}_x^H \mathbf{W}_g^a \right\|^2 | v_x \in \Gamma_g \right\}$;
8: $\quad [\sim, \Lambda] = sort(\mathbf{H}, ' descend')$;
9: $\quad$ **if** $|\Gamma_g|$ is odd **then**
10: $\quad\quad V_{g,i}^1 = \Lambda\left(i\right)$, $V_{g,i}^2 = \Lambda[i + \frac{|\Gamma_g|-1}{2}]$ for $1 \leq i \leq \frac{|\Gamma_g|-1}{2}$;
11: $\quad\quad V_{g,\frac{|\Gamma_g|+1}{2}}^1 = \Lambda\left(|\Gamma_g|\right)$;
12: $\quad$ **else**
13: $\quad\quad V_{g,i}^1 = \Lambda\left(i\right)$, $V_{g,i}^2 = \Lambda[\frac{i+|\Gamma_g|}{2}]$ for $1 \leq i \leq \frac{|\Gamma_g|}{2}$;
14: $\quad$ Calculate $\mathbf{w}_{g,n}^i$ according to (6);

Based on the above discussion, the union-based VUE-RB matching algorithm is proposed, including clustering phase and matching phase. In Algorithm 2, BD&VC algorithm is proposed for clustering phase, where each VUE is sequentially allocated to the optimal analog beam according to channel correlation. Specially, $\mathbf{w}_g^a$ may not be matched with VUEs. Considering the overhead of the digital precoder, such $\mathbf{w}_g^a$ is deleted by $\mathbf{w}_g^a$ to decrease $G_D$. The quantization precision of the analog precoder is set as $B = \lfloor \log_2(G_{BS}) \rfloor$ to ensure that $G_D \leq G_{BS}$ can always be satisfied [17]. Then, to make the VUEs in the same NOMA cluster have a certain difference of channel gain [18], VUEs is sorted according to path loss.

*Remark 1. BD&VC algorithm has the polynomial complexity. Specifically, the maximum complexity is* $\mathcal{O}\left(G_{BS} U\right)$ *from step 2 to 3, while the maximum complexity is* $\mathcal{O}(\sum_{g=1}^{G_{BS}} |\Gamma_g| \log |\Gamma_g|) \leq \mathcal{O}\left(G_{BS} U \log U\right)$ *from step 6 to 14.*

Cluster-RB matching has compatible definitions and properties with VUE-RB matching. Specifically, for $\Psi$, the VUE set $V = \{v_1, v_2, \ldots, v_U\}$ can be represented by the cluster set $\mathcal{N} = \{\mathcal{N}_{1,1}, \mathcal{N}_{1,2}, \ldots, \mathcal{N}_{g,n}, \ldots, \mathcal{N}_{G_D,|\mathcal{N}_{G_D}|}\}$.

Algorithm 3 describes the propsosed matching algorithm. In clustering phase, a series of minimal unions are formed by BD&VC algorithm, where the prior knowledge for matching, i.e. alternative and preference, is obtained. In matching phase, the largest stable unions in each RB are formed. Specifically, considering constraint (16c) and the multiplexing ability, a suitable cluster $\mathcal{N}_{g,n}$ is selected. Then, alternative and preference are utilized for $f_k$ to update $\Psi(f_k)$, until $(f_k, \Psi(f_k))$ cannot be blocked by any cluster. At this point, $\Psi(f_k)$ is regarded as the current largest stable union of $f_k$. Finally, the matching phase terminates when all VUEs are scheduled.

**Algorithm 3.** Union-based VUE-RB Matching Algorithm

**Require:** The input in **Algorithm 2**; threshold $\delta_{th}$.
**Ensure:** SPS period $K\tau_{RB}$; $\{\theta^k_{g,n}\}$; $\{\alpha^i_{g,n}\}$.

Init. $\Psi = \varnothing$; $k = 0$;
Run BD&VC algorithm;
**repeat**
  $c = 1$ and $k = k + 1$;
  $g = \arg\max_{l \in G_D} (|\mathcal{N}| - \sum_{i=1}^{k} \sum_{j=1}^{|N_l|} \theta^i_{l,j})$;
  $n = \arg\max_{j \in |\mathcal{N}_g|} ||\mathbf{h}^1_{g,j}||^2$;
  $\Psi(f_k) = \Psi(f_k) \cup \mathcal{N}_{g,n}$ and $\Psi(\mathcal{N}_{g,n}) = f_k$;
  **repeat**
    Form $\mathcal{R}$ for $\{\mathcal{N}_{g,n} | \Psi(\mathcal{N}_{g,n}) == \mathcal{N}_{g,n}, \mathcal{N}_{g,n} \in \mathcal{N}\}$ to find the most preferred $\mathcal{N}_{g',n'}$ for $(f_k, \Psi(f_k))$;
    **if** $\tilde{\delta}_{th}(f_k, \Psi(f_k) \cup \{\mathcal{N}_{g',n'}\}) < \delta_{th}$ or problem (26) is infeasible **then**
      $c = 0$;
    **else**
      $\Psi(f_k) = \Psi(f_k) \cup \mathcal{N}_{g',n'}$ and $\Psi(\mathcal{N}_{g',n'}) = f_k$;
      Update $\{\theta^k_{g,n}\}$, then record $\{\alpha^i_{g,n}\}$ and $\tilde{\delta}_{th}$ for $f_k$;
  **until** $c == 0$
  **if** $k > 1$ **then**
    $[\sim, ind] = \min\{\tilde{\delta}^1_{th}, \tilde{\delta}^2_{th}, \ldots, \tilde{\delta}^{k-1}_{th}\}$;
    Find the alternative-pair set $\{(\mathcal{N}_{g,n}, \mathcal{N}_{g,n'})\}$, where $\mathcal{N}_{g,n} \in \Psi(f_k)$, $\mathcal{N}_{g,n'} \in \Psi(f_{ind})$, $ind < k$;
    Judge for alternative pairs according to (28);
**until** $\forall v_u \in V$, $\Psi(v_u) \neq \{v_u\}$

### 3.3 Performance Analysis

In Algorithm 3, the number of proposals for unscheduled clusters is $N_1^k \leq \frac{1}{2}[(|N| - \sum_{i=1}^{k-1} |\Psi(f_i)|)^2 + |N| - \sum_{i=1}^{k-1} |\Psi(f_i)|] \leq \frac{|N|^2+|N|}{2}$, while the number

of proposals for scheduled clusters is $N_2^k \leq |\Psi(f_k)| \leq |\mathcal{N}|$. Hence, the upper bound of proposals for $f_k$ can be expressed as

$$\begin{aligned} N_1^k + N_2^k &\leq \max_{n=1,2,\ldots,|\mathcal{N}|} \{\frac{1}{2}(|\mathcal{N}| - n)^2 + \frac{1}{2}(|\mathcal{N}| - n) + n\} \\ &\leq \frac{1}{2}|\mathcal{N}|^2 - \frac{1}{2}|\mathcal{N}| + 1. \end{aligned} \tag{28}$$

For each proposal, $\mathcal{R}$ is formed by LLHR-PC algorithm, where the binary search is utilized. Hence, the number of searches to initiate a proposal is

$$|\mathcal{N}|(1 + \log \frac{1 - \delta_{th}}{\varepsilon_\delta}) \leq U(1 + \log \frac{1 - \delta_{th}}{\varepsilon_\delta}). \tag{29}$$

Combining with the complexity of BD&VC algorithm, the complexity of Union-based VUE-RB Matching Algorithm is

$$\begin{aligned} &\mathcal{O}(G_{BS} U \log U) + \mathcal{O}(|\mathcal{N}|(1 + \log \frac{1 - \delta_{th}}{\varepsilon_\delta}) K \sum_{k=1}^{K} (N_1^k + N_2^k)) \\ &= \mathcal{O}(U \log U) + \mathcal{O}(|\mathcal{N}|^3). \end{aligned} \tag{30}$$

## 4 Simulation Results

The performance in terms of SPS period of the mmWave-NOMA-based SPS strategy proposed in this paper is evaluated by simulations. For comparison, we consider the following five typical schemes to respectively show the performance of resource allocation, multiplexing, precoding: (1) "Greedy VUE-RB Matching", where LLHR-PC and BD&VC are also utilized, while VUEs and RBs are matched greedily until all VUEs can meet the QoS constraints in one SPS period [4]; (2) "Hybrid Precoding (HP) OMA", where the scheduling strategy is similar to the proposed scheme, but all VUEs are orthogonal in power domain.; (3) "Fully Analog Precoding (FAP) NOMA" [14], where only (4) is utilized for precoding; (4) "Strong user (SU) based HP NOMA" [17,18], where the HP scheme is similar to the proposed one, while the digital precoding vectors are calculated according to the normalized channel vectors of SU; (5) "Weak user (WU) based HP NOMA", where the digital precoding vectors are calculated according to the normalized channel vectors of WU.

Specifically, the simulation parameters are described as follows. CCF is set as $f_c = 63\,\text{GHz}$, and the aggregated system bandwidth is $\omega = 1\,\text{GHz}$ [6]. For the transmitting process, $P_t = 43\,\text{dBm}$, $\sigma_v = -174\,\text{dbm/Hz}$, $M_{BS} = 64$ and $G_{BS} = 16$. For $V_{g,n}^i$, the channel vector is generated by (1), where we assume the number of paths is $L = 3$, including the line-of-sight (LoS) path with the path loss exponent $\eta_1 = 4$ and the non-line-of-sight (NLoS) paths with $\eta_2 = \eta_3 = 5$. PRR is calculated by (15), where we assume: the slope parameter $\mu = 8$, the size of packets $L_{g,n}^i = 1200\,\text{bytes}$, short time slot $\tau_{RB} = 1/14\,\text{ms}$ [19]. Moreover, the road configuration for unban grid discussed in this paper is presented in

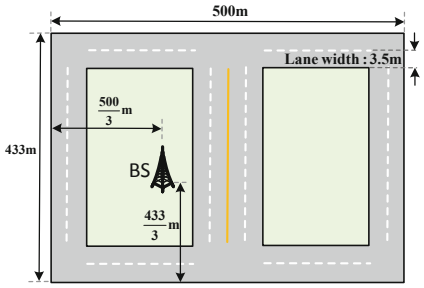


**Fig. 2.** Road configuration for urban grid.

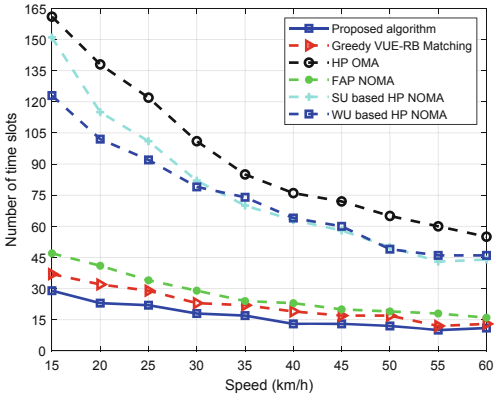


**Fig. 3.** Number of time slots in one SPS period against speed of vehicles.

Fig. 2 according to 3GPP eV2X systems defined in [6], where the car distance is $|\mathbf{v}^i_{g,n}| \times 2.5\,\mathrm{s}$ [4].

Figure 3 shows number of time slots in one SPS period against speed of vehicles from 15 km/h to 60 km/h. The packet of $v^i_{g,n}$ is successfully received only when $\delta^i_{g,n} \geq 99\%$. The density of VUE decreases when the speed increases, and thus, there are fewer clusters, leading to a shortening of SPS period. Moreover, it is intuitive that the proposed strategy works better than other five schemes, especially in a dense network.

Figure 4 shows SPS period, i.e. $K\tau_{RB}$, against PRR threshold from 80% to 99.999%, where the speed is 30 km/h. The SPS period increases as threshold increases. For "Greedy VUE-RB Matching" and "FAP NOMA" as well as the proposed algorithm, the systems can achieve a very short period when threshold is low. However, the period of "FAP NOMA" increases rapidly as threshold increases, since its space division multiplexing ability is limited. Additionally, the proposed algorithm always outperforms "Greedy VUE-RB Matching", since the properties of preference are utilized.

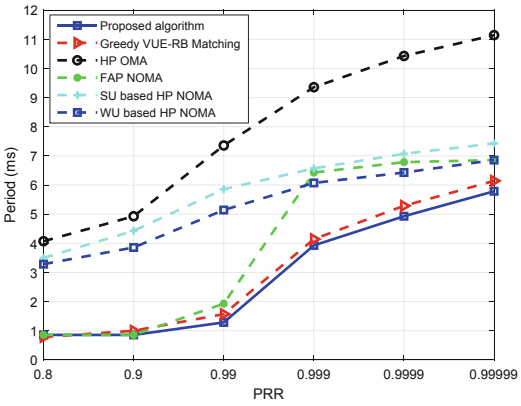


**Fig. 4.** SPS period against PRR threshold.

## 5 Conclusions

In this paper, we studied the SPS strategy in mmWave-NOMA-based eV2X systems, including hybrid precoding, user scheduling and resource allocation. The VUE-RB matching problem with peer effects was solved by the proposed union-based two-phase matching algorithm. Specifically, in clustering phase, BD&VC algorithm was designed to reduce the matching complexity; in matching phase, LLHR-PC algorithm was proposed to provide evaluation indicators for scheduling. Simulation results showed that the scheduling period of eV2X systems can be improved by the proposed SPS strategy compared with the conventional mmWave SPS schemes.

**Acknowledgment.** This work was supported by the Postgraduate Research & Practice Innovation Program of Jiangsu Province under grant number SJKY19_2285.

## References

1. Di, B., Song, L., Li, Y., Li, G.Y.: Non-orthogonal multiple access for high-reliable and low-latency V2X communications in 5G systems. IEEE J. Sel. Areas Commun. **35**(10), 2383–2397 (2017)
2. Study on enhancement of 3GPP Support for 5G V2X Services, Release 16, document 3GPP TR 22.886, December 2018
3. Study on NR Vehicle-to-Everything (V2X), Release 16, document 3GPP TR 38.885, March 2019
4. Wang, P., Di, B., Zhang, H., Bian, K., Song, L.: Cellular V2X communications in unlicensed spectrum: harmonious coexistence With VANET in 5G systems. IEEE Trans. Wireless Commun. **17**(8), 5212–5224 (2018)
5. Asadi, A., Müller, S., Sim, G.H., Klein, A., Hollick, M.: FML: fast machine learning for 5G mmWave vehicular communications. In: Proceedings of IEEE INFOCOM, Honolulu, HI, pp. 1961–1969 (2018)

6. Study on evaluation methodology of new vehicle-to-everything (V2X) use cases for LTE and NR, Release 15, document 3GPP, TR 37.885, December 2018
7. Giordani, M., Zanella, A., Zorzi, M.: Millimeter wave communication in vehicular networks: challenges and opportunities. In: Proceedings of IEEE MOCAST, Thessaloniki, pp. 1–6 (2017)
8. Sohrabi, F., Yu, W.: Hybrid digital and analog beamforming design for large-scale antenna arrays. IEEE J. Sel. Areas Commun. **10**(3), 501–513 (2016)
9. Zhang, D., Liu, Y., Dai, L., Bashir, A.K., Nallanathan, A., Shim, B.: Performance analysis of FD-NOMA-based decentralized V2X systems. IEEE Trans. Commun. **67**, 5024–5036 (2019). (in press)
10. Qian, L.P., Wu, Y., Zhou, H., Shen, X.: Non-orthogonal multiple access vehicular small cell networks: architecture and solution. IEEE Netw. **31**(4), 15–21 (2017)
11. Luo, F.L., Zhang, C.J.: Signal Processing for 5G: Algorithms and Implementations, pp. 143–166. Wiley, London (2016)
12. Wang, B., Dai, L., Gao, X., Hanzo, L.: Beamspace MIMO-NOMA for millimeter-wave communications using lens antenna arrays. In: Proceedings of IEEE VTC-Fall, Toronto, ON, pp. 1–5 (2017)
13. Wei, Z., Zhao, L., Guo, J., Ng, D.W.K., Yuan, J.: A multi-beam NOMA framework for hybrid mmWave systems. In: Proceedings of IEEE ICC, Kansas City, MO, pp. 1–7 (2018)
14. Cui, J., Liu, Y., Ding, Z., Fan, P., Nallanathan, A.: User selection and power allocation for mmWave-NOMA networks. In: Proceedings IEEE GLOBECOM, Singapore, pp. 1–6 (2017)
15. Wang, B., Dai, L., Wang, Z., Ge, N., Zhou, S.: Spectrum and energy-efficient beamspace MIMO-NOMA for millimeter-wave communications using lens antenna array. IEEE J. Sel. Areas Commun. **35**(10), 2370–2382 (2017)
16. Karadag, G., Gul, R., Sadi, Y., Coleri Ergen, S.: QoS-constrained semi-persistent scheduling of machine-type communications in cellular networks. IEEE Trans. Wireless Commun. **18**(5), 2737–2750 (2019)
17. Dai, L., Wang, B., Peng, M., Chen, S.: Hybrid precoding-based millimeter-wave massive MIMO-NOMA with simultaneous wireless information and power transfer. IEEE J. Sel. Areas Commun. **37**(1), 131–141 (2019)
18. Alsaba, Y., Leow, C.Y., Abdul Rahim, S.K.: Full-duplex cooperative non-orthogonal multiple access with beamforming and energy harvesting. IEEE Access **6**, 19726–19738 (2018)
19. Lee, K., Kim, J., Park, Y., Wang, H., Hong, D.: Latency of cellular-based V2X: perspectives on TTI-proportional latency and TTI-independent latency. IEEE Access **5**, 15800–15809 (2017)